Synthesis and application of a molecularly imprinted polymer for the voltammetric determination of famciclovir

ARTICLE *in* BIOSENSORS & BIOELECTRONICS · MARCH 2015

Impact Factor: 6.41 · DOI: 10.1016/j.bios.2014.10.024

4 AUTHORS, INCLUDING:

Nesrine Elgohary
The German University in Cairo
2 PUBLICATIONS **11** CITATIONS
SEE PROFILE

Rasha el nashar
Cairo University
37 PUBLICATIONS **305** CITATIONS
SEE PROFILE

Boris Mizaikoff
Universität Ulm
309 PUBLICATIONS **4,796** CITATIONS
SEE PROFILE

Biosensors and Bioelectronics 65 (2015) 108–114

Contents lists available at ScienceDirect

Biosensors and Bioelectronics

journal homepage: www.elsevier.com/locate/bios

Synthesis and application of a molecularly imprinted polymer for the voltammetric determination of famciclovir

Nesrine Abdelrehim El Gohary [a], Adel Madbouly [b], Rasha Mohamed El Nashar [a,b,*], Boris Mizaikoff [c]

[a] Pharmaceutical Chemistry Department, Faculty of Pharmacy and Biotechnology, The German University in Cairo, Cairo, Egypt
[b] Chemistry Department, Faculty of Science, Cairo University, Giza, Egypt
[c] Institute of Analytical and Bioanalytical Chemistry, University of Ulm, 89081 Ulm, Germany

ARTICLE INFO

Article history:
Received 15 August 2014
Received in revised form
29 September 2014
Accepted 9 October 2014
Available online 19 October 2014

Keywords:
Molecular imprinted polymers
MIPs
Famciclovir
Computational studies
Carbon paste electrode
and cyclic voltammetry

ABSTRACT

A molecularly imprinted polymer (MIP) was synthesized and applied as additive within a carbon paste electrode for the cyclic voltammetric determination of famciclovir (FCV). Complementary computational studies were performed to study the intermolecular interactions in the pre-polymerization mixture. Derived from the computational studies, four MIP ratios were synthesized and their performance was evaluated using equilibrium rebinding assays. The MIP with the highest binding capacity was selected. A linear response was obtained in the range of 2.5×10^{-6}–1.0×10^{-3} M with a limit of detection at 7.5×10^{-7} M. Finally, the developed MIP–voltammetry system was successfully applied for the determination of FCV in pure solutions and pharmaceutical preparations.

1. Introduction

Famciclovir (FCV) is a guanine analog antiviral prodrug that is converted by 1st pass metabolism into the active drug penciclovir. Chemically, FCV constitutes 2-[(acetyloxy) methyl]-4-(2-amino-9H-purin-9-yl) butyl acetate. It is successfully used for the treatment of herpes simplex virus (HSV-1), (HSV-2) and varicella zoster virus. More discussion regarding the mechanism of action of FCV has been given in the Supplementary information.

Several methods have been reported for the determination of FCV, such as reversed-phase liquid chromatography (RP-LC) (Mondal and Neeraja, 2013), LC–MS (Brock et al., 2012), liquid chromatography with mass spectrometric detection (LC–MS/MS) (Basu et al., 2011), capillary electrophoresis with electro-chemiluminescence (CE-ELC) (Ye and Chen, 2010), spectrophotometric determination (Reddy and Srikar, 2009), as well as potentiometric (Rezk and El Nashar, 2013) and voltammetric analysis (Chunzhe et al., 2006; Rajeev and Sanjay, 2012). To the best of our knowledge, there is no report published combining electrochemical studies of FCV with molecular imprinted polymers (MIP) as a selective modifier of carbon paste electrodes.

MIPs are artificial receptors providing highly specific complementary binding sites for a certain template in a cross-linked polymer network. Modern molecular imprinting technology was introduced by Wulff and Sarhan (1972) and the team of Mosbach (Arshady and Mosbach, 1981). The synthesis strategy involves the co-polymerization of a monomer and a cross-linker in the presence of a template molecule. After polymerization the template is extracted from the polymer matrix, thus ideally leaving selective recognition sites (i.e., 'imprints') for the template behind (Wang et al., 2014). Compared to natural bioreceptors MIPs offer a number of advantages, in particularly long-term storage stability, potential re-usability, resistance to microbial damage, facile integration into transducers (Karimian et al., 2014), low cost, ease of preparation, and finally, comparable affinity and recognition ability for the target substrate (Wang et al., 2014; Xie et al., 2009). MIPs have a wide range of applications including drug delivery systems (Ruela et al., 2014), stationary phases in HPLC analysis (T. Chen et al., 2014; J. Chen et al., 2014), solid phase extraction (Shaikh et al., 2014), capillary electrochromatography (CEC) (Liu et al., 2013) and sensors (Rizk et al., 2014).

Complementarily, electrochemical sensors offer small dimensions, low cost transducers, low detection limits and easy automation. Electrochemical sensors and biosensors for agricultural,

* Corresponding author at: Pharmaceutical Chemistry Department, Faculty of Pharmacy and Biotechnology, The German University in Cairo, NEW Cairo City, Egypt.
E-mail address: rasha.elnashar@guc.edu.eg (R.M. El Nashar).

http://dx.doi.org/10.1016/j.bios.2014.10.024
0956-5663/

environmental, food and pharmaceutical analyses have been increasing rapidly due to electrochemical behavior of drugs and biomolecules and partly due to advances in electrochemical measuring systems (Tajik et al., 2013, 2014).

The combination of MIPs with electrochemical analysis schemes is rather recent, and was predominantly used to combine the intrinsic properties of MIPs with selected electrochemical reactions, in order to improve the response of the electrode (Arvand and Fallahi, 2013; Gholivand and Torkashvand, 2011).

In this study, MIPs were synthesized for FCV with the aid of computer-based studies to optimize the synthesis route using methacrylic acid (MAA) as functional monomer, ethylene glycol dimethacrylate (EGDMA) as cross-linker and methylene chloride (DCM) as porogen. Batch adsorption experiments were performed to evaluate the MIP properties. Thereafter, the MIP with the highest binding capacity was incorporated as a modifier into carbon paste electrodes for enhancing the voltammetric determination of FCV. The use of carbon paste combined with MIPs offered several advantages such as ease of preparation, lower limits of detection, a wide usable concentration range and high selectivity and stability.

2. Materials and methods

2.1. Reagents and materials

All chemicals were of analytical grade and used without further purification, FCV reference standard was purchased from H and Y international group (China). The pharmaceutical preparations Famvir® (250 mg/tablet) (Novartis pharma) and Propencivir® (125 mg/tablet) (Bioriginal international group pharma) were purchased from the local market. MAA, EGDMA, 4-Vinyl pyridine (4-VP), 2,2′-azobisiso-butyronitrile (AIBN), graphite powder ($<20\ \mu m$) and paraffin oil were purchased from Sigma-Aldrich, Germany. The porogen DCM was of HPLC grade and purchased from Sigma, ultra pure water purified in purelab UHQ (ELGA) was used throughout this work. 0.04 M Britton–Robinson (BR) buffer, 0.04 M acetate buffer were used. 0.01 M FCV stock solutions were prepared in buffer solutions or ultrapure water and lower concentrations were prepared by appropriate dilutions.

2.2. Computational optimization and energy calculations

The Gaussian03 software package was used to study the binding interaction between the functional monomers (MAA/4-VP) and template molecules. The structures of monomer, template and template–monomer complexes were established using the gaussview software. All structures were optimized using Hartree–Fock theory with 6–31G(d) basis set.

The binding energy of template–monomer complexes, ΔE, were calculated via $\Delta E = E(\text{template–monomer complex}) - E(\text{template}) - nE(\text{monomer})$ following Roy et al. (2014). Consequently, an increasing value of the interaction energy between two molecular moieties indicates and increased stability of the complex formed between these moieties.

The polarizable continuum model (PCM) was applied to calculate the energy of complex, where the effect of solvent should be considered during energy calculations as it leads to changes in stability and energy of the template–monomer complexes in solvent phase compared to gaseous phase (Roy et al., 2014). In this model, the solvent is modeled as a polarizable continuum instead of individual molecules. The results obtained from computational study of template–monomer interaction provided the basis for selecting appropriate monomers and the choice of monomer–template ratio for synthesis of the MIPs.

Table 1
The chemical composition of the prepared MIPs.

	Template (mmol)	Functional monomer[a] (mmol)	Cross linker (mmol)	Porogen (ml)	Initiator (mmol)
MIP1	1	4	20	4	0.3
MIP2	1	4	40	4	0.3
MIP3	1	8	40	4	0.3
MIP4	1	4	40	4	0.3

[a] MAA was used as a functional monomer except in MIP4 where 4-VP was used.

2.3. Apparatus

Voltammetric measurements were performed in a three electrode cell using a CHI 802 B electrochemical analyzer (CH instruments, Inc., USA). CHI 150 saturated calomel electrode was used as a reference electrode, platinum wire 1.0 mm diameter was used as a counter electrode and a modified carbon paste was used as working electrode. UV-spectroscopic measurements were performed using Jasco V-530 UV/vis spectrophotometer (Japan). Incubation of MIPs with FCV solutions was done in an Eppendorf Thermomixer® (Germany).

2.4. Preparation of the molecularly imprinted polymer

The MIPs were prepared by bulk polymerization using the self-assembly approach (Arshady and Mosbach, 1981). The chemical composition of the synthesized MIPs is summarized in Table 1. More details regarding the synthesis of the polymers has been given in the Supplementary information.

2.5. Equilibrium binding assays

Equilibrium rebinding experiments were carried out for the MIPs and their corresponding NIPs by adding 2 mL of 1.0×10^{-4} M solution of FCV prepared in pure H_2O over 20 mg of MIP or NIP in a 2 mL Eppendorf tube. The tubes were located in an Eppendorf thermomixer and left to shake for 24 h at room temperature followed by centrifugation at 14,000 rpm for 20 min. The resulting supernatant was filtered using a 0.22 μm Whatman syringe filter and the amount of FCV in the clear supernatant was determined by UV/vis. spectrophotometry at 304 nm. The same experiment was conducted using 1.0×10^{-4} M FCV prepared in 0.04 M acetate buffer, pH 5. To determine the binding isotherms and to perform Scatchard analysis for MIP1, 20 mg of MIP1 and NIP1 were incubated with 2 mL solutions of FCV prepared in pure H_2O with concentrations ranging from 1.0×10^{-5} to 1.0×10^{-2} M at the same conditions as stated before; all experiments were done in duplicates.

The amount of FCV bound to the polymers was determined by $Q=[(C_i-C_f)\times V_s\times 1000]/M$, where Q is the binding capacity of the polymer in (μM/g), C_i is the initial FCV concentration in (μM/mL), C_f is the final free FCV concentration at equilibrium in (μM/mL), V_s is the volume of sample solution tested (mL) and M is the mass of polymer used in (mg) (Moreira et al., 2011); the imprinting factor (IF) was calculated as Q_{MIP}/Q_{NIP}.

The Scatchard plot was constructed following $Q/[F] = -(Q/K_d) + (Q_{max}/K_d)$, where Q is the binding capacity of the polymer in (μM/g), $[F]$ is the final free FCV concentration at equilibrium in (mM), K_d is the dissociation constant and Q_{max} is the maximum apparent binding amount, the values of K_d and Q_{max} can be calculated from the slope and intercept of the linear line plotted in $Q/[F]$ vs. Q (Wang et al., 2011).

2.6. Electrode fabrication

Bare carbon paste electrodes (CPE) were prepared by mixing 0.5 g of fine graphite powder with 0.2 g of paraffin oil in a mortar. The paste was packed into one end of a plastic syringe of diameter 5 mm and an electrical contact was made using a copper wire. The electrode surface was polished using a wet filter paper. The surface was regenerated after each set of electrochemical experiments by removing a thin layer of paste from the surface. The modified carbon paste electrode (MIP–CPE) was prepared by mixing MIP with graphite powder at specified percentages (1%, 5%, 10%, 15% and 20%) (Aswini et al., 2014; Moghaddam, 2011) and mixing to homogeneity for 10 min. Then, paraffin oil was added and the components were mixed together for another 10 min. The NIP modified CPE (NIP–CPE) was prepared by following the same procedure at the optimum composition obtained for (MIP–CPE).

2.7. Analytical evaluation

Cyclic voltammograms were recorded in the potential range of −0.5 to 1.5 V at a scan rate of 0.13 V s^{-1} after 30 s of accumulation time at open circuit potential. All solutions were purged with argon gas for 2 min before measurements. All electroanalytical measurements were performed at room temperature (25 ± 2 °C).

Each set of experiments was performed with the same electrode surface, where after each measurement the electrode was immersed in distilled water for 30 s then it was scanned in the supporting electrolyte solution from −0.5 to 1.5 V till the background current returned to normal.

Finally, the MIP–CPE was used for the quantification of FCV in pure solutions and dosage forms (Famvir® 250 mg/tablet and Propencivir® 125 mg/tablet) using the standard additions method. For the assay of tablets, five tablets were ground and powdered in a mortar. Then, aliquots were dissolved in 100 mL to prepare a 0.01 M stock solution. Appropriate dilutions in a 0.04 M acetate buffer pH 5, were made to prepare a calibration series ranging from 2.5×10^{-6} to 1.0×10^{-4} M.

3. Results

3.1. Computational studies

Experimentally testing the many variables involved in MIP synthesis is both time-consuming and expensive. This provides enough motivation for the optimization of experimental conditions using computer-based methods (Mahony et al., 2005; Meier et al., 2012; Nicholls et al., 2009; Wei et al., 2006, 2007). Since the structure of the template–monomer complexes formed in the pre-polymerization solution is ideally preserved in the synthesized polymer, only interactions between the template and the monomer that occurred in the presence of porogen were considered in the computational study (Subrahmanyam and Piletsky, 2009).The influence of the cross-linking agent was neglected in the present study in order to simplify calculations (Liu et al., 2007; Zolek et al., 2011). Optimization of the structures of the template and monomer molecules via calculation of the minimized energies of their respective structures was carried out. Optimized molecular structures of selected monomers (MAA/4-VP) and of the template are shown in Fig. 1.

Table 2 summarizes the calculated interaction energies for complexes formed between FCV and functional monomers in the gaseous as well as solvent (DCM) phase. The obtained results in both the gaseous phase and solvent reveal that the (FCV/MAA) complex is more stable than the (FCV/4-VP) complex, and that the optimum ratio of interaction between FCV and MAA is (1:4). Moreover, in solution phase, order of interaction energy is quite similar to that obtained in gaseous phase, which suggests that binding between template and monomer is strong enough to persist also in solution phase (Roy et al., 2014). The structures of the most stable complexes formed between (FCV/MAA), (FCV/4-VP) are shown in Fig. 1. The study was conducted for a ratio of (1:4) between (FCV/MAA) and (1:2) for (FCV/4-VP); these ratios maximize the formation of hydrogen bonding interactions between the template and the monomers (Zolek et al., 2011). Therefore, the polymers in this work were synthesized with the optimized ratio (1:4) between template and monomer, which was expected to yield the highest efficiency.

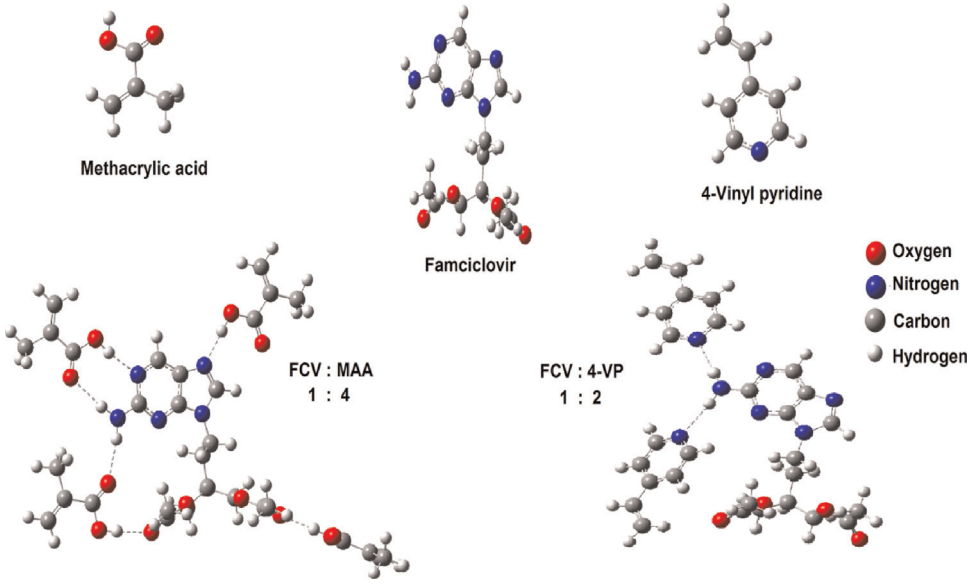

Fig. 1. Optimized structures of the template (FCV), monomers (MAA, 4-VP) and the most stable complexes formed between (FCV/MAA), (FCV/4-VP).

Table 2
Computational study of interaction energy between chosen monomer and template complex in gaseous and solvent phase.

Name of complex	Gaseous phase		Solvent phase (DCM)	
	ΔE (Hartree)[a]	ΔE (kJ/mol)	ΔE (Hartree)	ΔE (kJ/mol)
FCV/MAA	−0.0201	−52.7725	−0.0141	−37.0195
FCV/$(MAA)_2$	−0.0337	−88.4793	−0.0235	−61.6992
FCV/$(MAA)_3$	−0.0512	−134.4256	−0.0353	−92.6801
FCV/$(MAA)_4$	−0.0698	−183.2599	−0.0473	−124.1861
FCV/4-VP	−0.0083	−21.7916	−0.0048	−12.6024
FCV/$(4\text{-VP})_2$	−0.0170	−44.6335	−0.0099	−25.9924

[a] 1 Hartree = 2625.5 kJ/mol.

3.2. Equilibrium rebinding and Scatchard analysis

The results of incubating the polymers in a 1.0×10^{-4} M FCV solution prepared in pure H_2O and in a 1.0×10^{-4} M FCV prepared in 0.04 M acetate buffer, pH 5, are shown in Table S1. It is clear from the results that the polymers prepared with MAA as functional monomer showed higher binding capacities than the one prepared with 4-VP, which may be due to the stronger hydrophobic and electrostatic interactions between MAA and FCV in a polar environment (Shekarchi et al., 2013). This is also in line with the computational prediction suggesting that the (FCV/MAA) complex is more stable than the (FCV/4-VP) complex. Generally, the performance of the polymers prepared with MAA was slightly better in pure H_2O, than in, 0.04 M acetate buffer pH 5. However, for MIP4, the polymer prepared with 4-VP, the opposite was observed, i.e., the binding capacity was higher in the buffer solution, where the pH was slightly lower than the pKa of 4-VP. Hence, it is hypothesized that 4-VP was partially ionized, which may result in more pronounced interactions with FCV. More discussion has been provided in the Supplementary information.

MIP1 was selected for further examination, as it showed maximum binding capacity of all prepared MIPs. MIP1 was incubated with different concentrations of FCV solutions prepared in H_2O.

The binding isotherms in Fig. 2A show that at low concentrations small differences in the values of MIP1 and NIP1, yet, at high concentrations noticeable differences were observed, i.e., more FCV was adsorbed by MIP1 compared to NIP1.

The rebinding data were further processed using Scatchard analysis (Fig. 2B). Two distinct sections are evident within the plot, thus indicating that the affinities of the binding sites in both MIP1 and NIP1 are heterogeneous and can be approximated by two dissociation-constants corresponding to the high and low affinity binding sites for both polymers, respectively (T. Chen et al., 2014; J. Chen et al., 2014). For MIP1, the values of Q_{max} are 67.41 and 498.42 (μM/g) for high affinity and low affinity binding sites, respectively; the values of K_d for the high affinity and low affinity sites are 0.035 and 0.896 (mM), respectively. For NIP1, the values of Q_{max} are 57.48 and 375.65 (μM/g) for high affinity and low affinity binding sites, respectively; the values of K_d for the high affinity and low affinity sites are 0.036 and 0.77 (mM), respectively. The Q_{max} for the MIP was higher than the NIP in both the high affinity and low affinity regions, while the value of the K_d for the high affinity region was almost the same for both the MIP and the NIP and the value of the K_d for the low affinity region was slightly higher for the MIP.

3.3. Electrochemical behavior of famciclovir

The electrochemical study of a 5.0×10^{-5} M standard FCV solution in a pH 5, 0.04 M acetate buffer over the swept potential range revealed the presence of a well defined oxidation peak at +1.19 V (O_1) in the forward scan. After switching the potential to cathodic sweep in the reverse scan a reduction peak appeared at −0.41 V (R) and in the second anodic sweep another oxidation peak appeared at +0.7 V (O_2).

When the cyclic voltammograms were recorded to the potential before E_{O1}, that is to say the forward anodic scan was stopped before reaching +1.19 V, no reduction peak (R) or oxidation peak (O_2) appeared. Multiple cyclic voltammograms recorded in the range of −0.5 to 1.5 V showed a decrease in O_1 peak current with increasing the number of scans, while the peak current of (R) and

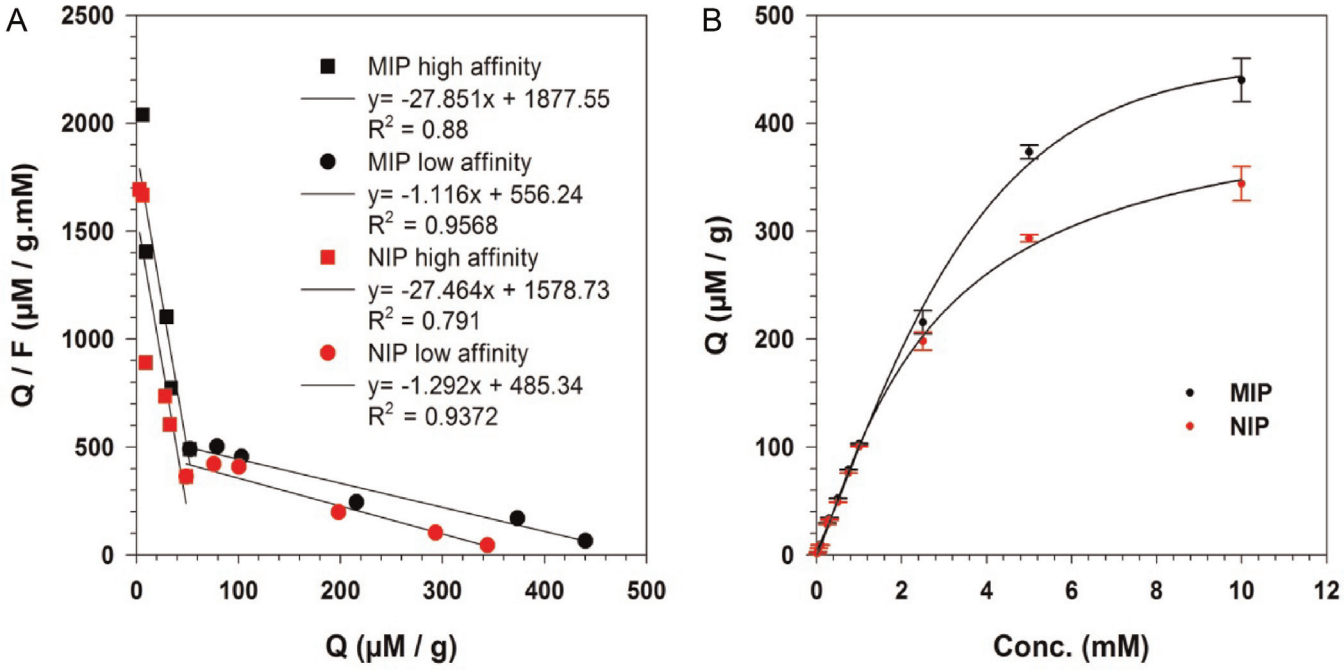

Fig. 2. (A) Binding isotherm of MIP1 and NIP1. (B) The results of Scatchard analysis for MIP1 and NIP1.

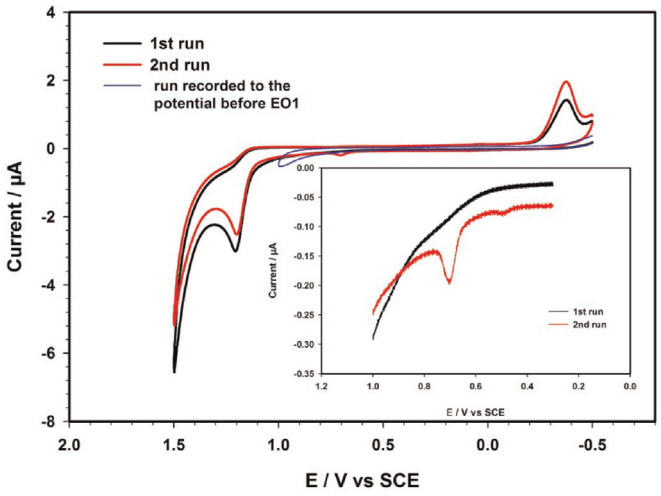

Fig. 3. Cyclic voltammograms of 5.0×10^{-5} M FCV at MIP–CPE in 0.04 M acetate buffer, pH 5, scan rate 0.13 V s^{-1}, showing two successive runs and a run recorded to the potential before EO_1, the inset figure shows a closer look at the O_2 peak in the two successive runs.

(O_2) increased. These results indicate that (R) and (O_2) peaks are due to chemical follow-up reactions after the first oxidation (O_1) (Ashrafi et al., 2013); the results are shown in Fig. 3.

The oxidation peak (O_1) is probably due to the oxidation of the 2-aminopurine ring in FCV to the corresponding 2-amino-8-oxypurine, mechanism is shown in Scheme 1; this mechanism has been reported before for aminopurines and for similar antiviral drugs (Dogan-Topal et al., 2013; Shah et al., 2013; Yao and Musha, 1979).

3.4. Parameter optimization

3.4.1. Carbon paste electrode composition

Different MIP modified electrodes were prepared by varying the percentage of MIP-content by weight (1%, 5%, 10%, 15% and 20%). The amount of binder was kept constant at 0.2 g providing for reproducible electrode properties. The electrode response was recorded after 30 s insertion in 5.0×10^{-5} M FCV solution. The response of the electrode increased by increasing the MIP content from 1% to 5%; thereafter, by further increasing the MIP content the response decreased. It was observed that the optimum response was obtained for MIP–CPEs containing 5% MIP. The corresponding results are shown in Fig. S1A. The response of the optimized MIP–CPE is clearly higher than the bare CPE and the NIP–CPE containing 5% NIP, Fig. S1B. In summary, using a 5% (MIP–CPE) results in an increase of the oxidation peak current, which in turn is anticipated to yield a decrease of the detection limit for FCV. More discussion has been provided in the Supplementary information.

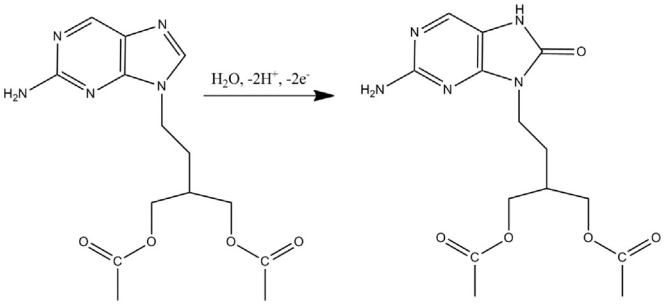

Scheme 1. Electrochemical oxidation of FCV at MIP modified CPE.

3.4.2. Effect of pH and supporting electrolyte

A series of FCV 5.0×10^{-5} M standard solutions in 0.04 M Britton–Robinson (BR) buffer covering the pH range (2–12) were prepared to determine the optimum pH of the supporting electrolyte for analysis, Fig. S2A and B. The effect of different buffer solutions was also studied.

An oxidation peak was observed starting pH 2 up to pH 10; above pH 10 the peak disappeared. As the pH of the solution was gradually increased, the oxidation peak potential for FCV shifted towards less positive values, which suggests the involvement of protons in the reaction (Arvand and Fallahi, 2013). Maximum peak current was observed for FCV solutions prepared in pH (3–6). Above pH 6, the peak current started to decrease until the oxidation peak completely disappeared at pH > 10.

A well-defined reduction peak for FCV started to appear in FCV solution of pH 4 and reached a maximum peak current at pH 6. Above pH 6, the reduction peak completely disappeared. The reduction peak shifted towards more negative potentials as the pH of the solution was increased which suggests the participation of protons in the reduction process.

The effect of different supporting electrolytes was studied using 0.04 M phosphate buffer pH 6, 0.04 M acetate buffer pH 4 and 0.04 M acetate buffer pH 5. The results were compared to those obtained in 0.04 M Britton–Robinson (BR) buffer pH 5 and 6.

The optimum response for both oxidation and reduction peaks was obtained in 0.04 M acetate buffer pH 5; hence, this buffer was selected as the supporting electrolyte for all the subsequent studies. Over the pH range of 2–7, the oxidation peak potential provided a linear response vs. pH, Fig. S2C. The corresponding linear calibration function is described as *Epa* (V) = −0.0474 pH + 1.4401 with $R^2=0.9858$.

For the reduction peak potential over the pH range (4–6), also a linear relationship was also obtained (Fig. S2C) following *Epc* (V) = −0.05 pH − 0.13 with $R^2=1$.

The slopes are close to the theoretical value of 0.059 V/pH; hence, it is safe to assume that an equal number of protons and electrons are involved (Sanghavi et al., 2014).

3.4.3. Effects of the scan rate

The effect of change of scan rate on both the oxidation (O_1) and reduction (R) peak currents for a 5.0×10^{-5} M FCV standard solution was investigated in the range of (0.01–0.45 V s^{-1}), Fig. S3A. The value of the oxidation peak current increased as the scan rate increased and it was found that it is linearly dependent on the square root of the scan rate in the range of 0.01–0.25 V s^{-1} according to *Ipa* (µA) = 0.1361 + 0.1702$\upsilon^{1/2}$ (mV s^{-1}); $R^2=0.9947$, which is typical for a diffusion controlled process (Abdel Razak, 2004). It was found that between the range of 0.03 and 0.17 V s^{-1} the oxidation peak current was linearly dependent on both the scan rate and square root of the scan rate, according to *Ipa* (µA) = 0.8479 + 0.0096υ (mV s^{-1}); $R^2=0.9817$, *Ipa* (µA) = 0.0442 + 0.1817$\upsilon^{1/2}$ (mV s^{-1}); $R^2=0.9955$ respectively, which suggests the involvement of an adsorption process at the electrode surface along with diffusion (Mahanthesha et al., 2010). Fig. S3B and C show the plot of I_p vs. υ and the plot of I_p vs. $\upsilon^{\frac{1}{2}}$, respectively.

The value of the reduction peak current also increased as the scan rate was increased till scan rate 0.13 V s^{-1}, with further increase in the scan rate the reduction peak current decreased and the shape of the peak was distorted at higher scan rates. More details has been provided in the Supplementary information.

A scan rate of 0.13 V s^{-1} was finally selected for subsequent studies where the response of the (MIP–CPE) was adequate and the shape of both the oxidation peak (O_1) and the reduction peak (R) was well defined.

3.4.4. Effect of accumulation time and accumulation potential

The effect of the accumulation time on a 5.0×10^{-5} M FCV standard solution was varied from 10 s to 120 s, it was found that the maximum response for the (O_1) peak was obtained after 30 s accumulation after that there was no enhancement of peak current. Hence, 30 s was selected for accumulation of FCV.

Keeping the accumulation time at 30 s at a concentration of 5.0×10^{-5} M FCV, the accumulation potential was varied in the range of −0.5 V to 1.5 V at 0.5 V increments. It was found that there was no significant difference in the peak current when compared to accumulation at open circuit conditions; hence, no accumulation potential was applied to the electrode.

3.5. Calibration function, reproducibility and precision

As the response of the oxidation peak (O_1) was significantly higher than the reduction peak (R), it was chosen for quantitative determination of FCV.

At optimum conditions for analysis, the relationship between the oxidation peak current and the concentration of FCV was studied using cyclic voltammetry, Fig. S4. It was found to be linear in the range from 2.5×10^{-6} M to 1.0×10^{-3} M. The limit of quantification (LOQ) was 2.5×10^{-6} M and the limit of detection (LOD) was calculated using LOD = 3S/m, where S is the standard deviation of the peak current of blank (n = 5) and m is the slope of the calibration curve (Gholivand et al., 2014; Shah et al., 2013), and was determined to be 7.5×10^{-7} M. To determine the repeatability of the response of the electrode, the response towards a 5×10^{-5} M FCV solution was recorded using six different surfaces of the same electrode, the relative standard deviation (RSD) was 2.27%. For studying the reproducibility, three (MIP–CPE) containing 5% MIP were prepared and their response towards a 5×10^{-5} M FCV solution was recorded (Afkhami et al., 2013) determining a RSD of 3.85%. These values for repeatability and reproducibility are suitable for routine quality control analysis of pharmaceutical compounds in their dosage forms (Gholivand and Torkashvand, 2011).

3.6. Interference effects

The selectivity of the (MIP–CPE) was examined in the presence of several interfering substances of close structure to FCV and excipients. Cyclic voltammograms for a 5.0×10^{-5} M solution of FCV were recorded in the absence and the presence of different concentrations (5.0×10^{-5}, 5.0×10^{-4} and 5.0×10^{-3} M) of the interfering substances (Kong et al., 2014). The results are shown in Table S2. In all cases when the interfering substance was present in an equimolar concentration to the analyte, the change in current response was negligible. When the concentration of the interferents was 10 times that of the analyte, there was no significant change in the current response, i.e., the change in current response was less than 5%. However, when the concentration of histidine and tryptophan was 100 times that of the analyte, the change in the current response was 100%, indicating that these amino acids may interfere with the determination of FCV. However, this concentration level of histidine and tryptophan (5.0×10^{-3} M) is much higher than the normal levels found in biological samples, which confirms that the electrode could be used to measure FCV in these samples without being affected. The antiviral drug lamivudine also caused considerable interference, i.e., 20.4% change in current response, when its concentration was 100 times that of the analyte, this concentration for lamivudine (5.0×10^{-3} M) is much higher than the peak plasma concentration reported for lamivudine (Bruno et al., 2001), accordingly, the electrode could be used to measure FCV in plasma samples of patients who might be taking lamivudine concomitantly with FCV.

3.7. Analytical applications

The (MIP–CPE) was used in the quantification of FCV in its pure solutions and dosage forms (Famvir® 250 mg/tablet and Propencivir® 125 mg/tablet) using the standard additions method. Results are shown in Table S3. The recoveries are in the range of 99.20–101.52% for the pure solutions, (99.01–104.00%) for (Famvir® 250 mg/tablet) and (98.50–102.30%) for (Propencivir® 125 mg/tablet). These values suggest a high degree of accuracy for the developed method.

The developed method was compared with a standard reference method (Rezk and El Nashar, 2013) to determine if there were any significant differences between the two methods. The obtained results are summarized in Table S3. A Student t-test and F-test were performed on the results to statistically examine the validity of the obtained results. The calculated t values were less than the tabulated t values at 95% confidence level, showing that there were no significant differences between the results obtained using the two methods. Also, the results of the F-test at the 95% confidence level reveal the precision of the developed method in comparison to the reference method.

4. Conclusions

The proposed sensor based on MIP-modified carbon paste electrodes offers an easy-to-use technique for the determination of famciclovir in standard drug solutions and in pharmaceutical formulations due the rapid response time, ease of construction and use, low cost, precise results, high sensitivity and selectivity, and direct applicability to quantitatively determine famciclovir in complex matrices without prior sample preparation or separation.

Acknowledgments

The authors would like to acknowledge Florian Meier at the Institute of Analytical and Bioanalytical Chemistry, University of Ulm, Germany for valuable advice. The authors would also like to acknowledge Assoc. Prof. Dr. Khaled Abou Aisha, Faculty of Pharmacy and Biotechnology, German University in Cairo, Egypt for his assistance.

Appendix A. Supplementary material

Supplementary data associated with this article can be found in the online version at http://dx.doi.org/10.1016/j.bios.2014.10.024.

References

Abdel Razak, O., 2004. J. Pharm. Biomed. Anal. 34, 433–440.
Afkhami, A., Ghaedi, H., Madrakian, T., Ahmadi, M., Mahmood-Kashani, H., 2013. Biosens. Bioelectron 44, 34–40.
Arshady, R., Mosbach, K., 1981. Die Makromol. Chem. 182, 687–692.
Ashrafi, A.M., Gumustas, M., Vytras, K., Nematollahi, D., Uslu, B., Miky-sek, T., Jirasko, R., Ozkan, S.A., 2013. Electrochim. Acta 109, 381–388.
Aswini, K.K., Mohan, A.M., Biju, V.M., 2014. Mater. Sci. Eng.: C 37, 321–326.
Basu, S., Sahu, R., Velamuri, R., Honrao, C., Basit, A., Surve, P., Sarode, S., Nayak, S., Patel, V.B., Vangala, S., 2011. J. Pharm. Res 4, 3738–3742.
Brock, A.P., Isaza, R., Hunter, R.P., Richman, L.K., Montali, R.J., Schmitt, D.L., Koch, D. E., Lindsay, W.A., 2012. Am. J. Vet. Res 73, 1996–2000.
Bruno, R., Regazzi, M.B., Ciappina, V., Villani, P., Sacchi, P., Montagna, M., Panebianco, R., Filice, G., 2001. Clin. Pharmacokinet. 40, 695–700.
Chen, J., Bai, L.Y., Liu, K.F., Liu, R.Q., Zhang, Y.P., 2014. Int. J. Mol. Sci. 15, 574–587.
Chen, T., Gu, J., Wang, H., Yuan, G., Chen, L., Xu, X., Xiao, W., 2014. Chromatographia 77, 893–899. http://dx.doi.org/10.1007/s10337-014-2691-z.
Chunzhe, L., Hainan, L., Donghai, P., Guifen, W., 2006. J. Instrum. Anal. 25, 102–105.

Dogan-Topal, B., Bozal-Palabiyik, B., Uslu, B., Ozkan, S.A., 2013. Sens. Actuat. B: Chem 177, 841–847.
Gholivand, M.B., Shamsipur, M., Dehdashtian, S., Rajabi, H.R., 2014. Mater. Sci. Eng.: C 36, 102–107.
Gholivand, M.B., Torkashvand, M., 2011. Talanta 84, 905–912.
Karimian, N., Turner, A.P., Tiwari, A., 2014. Biosens. Bioelectron 59, 160–165.
Kong, Y., Shan, X., Ma, J., Chen, M., Chen, Z., 2014. Anal. Chim. Acta 809, 54–60.
Liu, X., Zong, H.Y., Huang, Y.P., Liu, Z.S., 2013. J. Chromatogr. A 1309, 84–89.
Liu, Y., Wang, F., Tan, T., Lei, M., 2007. Anal. Chim. Acta 581, 137–146.
Mahanthesha, K.R., Swamy, B.K., Pai, K.V., Chandra, U., Sherigara, B.S., 2010. Int. J. Electrochem. Sci. 5, 1962–1971.
Mahony, J.O., Nolan, K., Smyth, M.R., Mizaikoff, B., 2005. Anal. Chim. Acta 534, 31–39.
Meier, F., Schott, B., Riedel, D., Mizaikoff, B., 2012. Anal. Chim. Acta 744, 68–74.
Moghaddam, H.M., 2011. Int. J. Electrochem. Sci. 6, 6557–6566.
Mondal, P., Neeraja, B., 2013. Pharm. Lett. 5, 320–325.
Moreira, F.T., Freitas, V.A., Sales, M.G., 2011. Microchim. Acta 172, 15–23.
Nicholls, I.A., Andersson, H.ÍS., Charlton, C., Henschel, H., Karlsson, B.R.C., Karlsson, J. G., O'Mahony, J., Rosengren, A.M., Rosengren, K.J., Wikman, S., , 2009. . Biosens. Bioelectron 25, , 543–-552.
Rajeev, J., Sanjay, S., 2012. Glob. J. Anal. Chem 3, 1.
Reddy, B.A., Srikar, A., 2009. J. Pharm. Sci. Technol 1, 36–39.
Rezk, M.S., El Nashar, R.M., 2013. Bioelectrochemistry 89, 26–33.
Rizk, M., Toubar, S.S., Sayour, H.E.E.-D., Mohamed, D., Touny, R.M., 2014. Eur. J. Chem. 5, 18–23.
Roy, E., Patra, S., Madhuri, R., Sharma, P.K., 2014. Talanta 120, 198–207.
Ruela, A.ÑL.ÕM., Figueiredo, E.C., Pereira, G.R., 2014. Chem. Eng. J. 248, 1–8.
Sanghavi, B.J., Kalambate, P.K., Karna, S.P., Srivastava, A.K., 2014. Talanta 120, 1–9.
Shah, B., Lafleur, T., Chen, A., 2013. Faraday Discuss. 164, 135–146.
Shaikh, H., Memon, N., Bhanger, M.I., Nizamani, S.M., Denizli, A., 2014. J. Chromatogr. A 1337, 179–187.
Shekarchi, M., Pourfarzib, M., Akbari-Adergani, B., Mehramizi, A., Javanbakht, M., Dinarvand, R., 2013. J. Chromatogr. B 931, 50–55.
Subrahmanyam, S., Piletsky, S.A., 2009. In: Potyrailo, R.A., Mirsky, V.M. (Eds.), Combinatorial Methods for Chemical and Biological Sensors. Springer, New York, pp. 135–172.
Tajik, S., Taher, M.A., Beitollahi, H., 2013. Sens. Actuat. B: Chem 188, 923–930.
Tajik, S., Taher, M.A., Beitollahi, H., 2014. Sens. Actuat. B: Chem 197, 228–236.
Wang, B., Wang, Y., Yang, H., Wang, J., Deng, A., 2011. Microchim. Acta 174, 191–199.
Wang, Z., Li, J., Xu, L., Feng, Y., Lu, X., 2014. J. Solid State Electrochem. 18, 2487–2496.
Wei, S., Jakusch, M., Mizaikoff, B., 2006. Anal. Chim. Acta 578, 50–58.
Wei, S., Jakusch, M., Mizaikoff, B., 2007. Anal. Bioanal. Chem. 389, 423–431.
Wulff, G., Sarhan, A., 1972. Angew. Chem. – Int. Ed. (Conf. Proc.) 11, 341.
Xie, C., Li, H., Li, S., Wu, J., Zhang, Z., 2009. Anal. Chem. 82, 241–249.
Yao, T., Musha, S., 1979. Bull. Chem. Soc. Japan 52, 2307–2311.
Ye, H.Z., Chen, G.N., 2010. J. Anal. Sci. 26, 621–625.
Zolek, T., Lulinski, P., Maciejewska, D., 2011. Anal. Chim. Acta 693, 121–129.